Second-Harmonic Generation by Ferroelectric Microparticles in Aerogels

S. Lisinski,*,† D. Schaniel,‡ L. Ratke,† and Th. Woike‡

Institute of Space Simulation, German Aerospace Center DLR, Linder Höhe, D-51170 Köln, Germany, and Institute of Mineralogy and Geochemistry, University of Cologne, Zülpicher Str.49 b, D-50674 Köln, Germany

Received December 16, 2005

The synthesis and preparation of aerogels and xerogels loaded with micrometer-sized ferroelectric particles of $BaTiO_3$ and $KNbO_3$ is described. We show that these composite aerogels and xerogels exhibit nonlinear optical properties, especially second-harmonic generation at an incident wavelength of 1064 nm.

Introduction

The nonlinear optical properties of ferroelectric crystals such as $KNbO_3$, $BaTiO_3$, and $LiNbO_3$ are exploited in many applications.[1] The use of single crystals for nonlinear optical applications such as second-harmonic generation (SHG) is well studied.[2] $KNbO_3$ and $LiNbO_3$ are useful frequency doubling crystals as phase-matching conditions are met by a suitable choice of the light polarization and propagation direction. In $BaTiO_3$ single crystals, on the other hand, the phase-matching condition cannot be fulfilled because of the incompatibility of the refractive indices. Here, so-called quasi phase matching is achieved by arranging 180° domains in a periodic grating with the grating period equal to the coherence length.[3] Although powder SHG was used to classify nonlinear optical materials,[4] powders were generally believed to have too low efficiencies for real applications. A further problem imposed by powder samples is their handling and possible tailoring of optical components. However, in recent years, interest in the nonlinear optical properties of powders was regained as unexpected high efficiencies for frequency conversion[5,6] and random lasers were detected.[7] By embedding the powders or polycrystalline particles in a transparent, shapeable matrix, their exploitation seems possible. Suitable transparent materials are aerogels or xerogels. The preparation of transparent silica aerogels by a sol−gel routine is state-of-the-art.[8] The sol−gel preparation of aero- or xerogels starts from a solution of alkoxides such as tetramethyl orthosilicate (TMOS), tetraethyl orthosilicate (TEOS) in alcohol (methyl or ethyl alcohol), water, and an acid or base catalyst. Waterglass gels are prepared from sodium waterglass, water, and a catalyst like hydrochloric or acetic acid. In both cases, the solution starts to form nanoparticles (pure silica or sodium silicate) which eventually build a three-dimensional network and thus lead to a gelation of the solution. After gelation, an aerogel is obtained by supercritical drying of the wet gel and a xerogel by ambient pressure drying. Silica or waterglass aerogels prepared by this routine consist of particles with a size of a few nanometers in diameter and with pore sizes of about 10 nm. The pore fraction in these aerogels can vary between 85 and 99%, depending on the process conditions and the sol composition. The pore fraction in xerogels typically is around 50%. The aerogels and xerogels prepared by our routines are transparent in the wavelength range of around 400−2500 nm (see below). We have chosen aerogels and xerogels as matrix for the ferroelectrical particles because their production is easy and expeditious, they are transparent in the visible to infrared spectral range, which is important for optical applications, and they allow for a homogeneous distribution of the particles in the aerogel matrix. Thus, aerogels and xerogels are interesting candidates for the incorporation of ferroelectric micrometer-sized particles into the gel network to investigate their nonlinear optical properties. Here, we demonstrate that aerogels and xerogels loaded with $BaTiO_3$ or $KNbO_3$ particles having sizes of 0.5−12 μm exhibit second-harmonic generation.

Experimental Section

Particle Characterization. $BaTiO_3$ was obtained as powder from Alfa Aesar and $KNbO_3$ was received from FEE Idar-Oberstein as large single crystals, which were milled manually to a fine powder. First, the powders were investigated by scanning electron microscopy (SEM, LEO 1530 VP). Figures 1a and 2a show the SEM results for the $BaTiO_3$ and $KNbO_3$ particles, respectively. While the $BaTiO_3$ particles have a typical size of around 1 mm and a spherical shape, the $KNbO_3$ particles have a broader size distribution. To determine the size distribution more quantitatively, we

* To whom correspondence should be addressed. E-mail: Susanne.Lisinski@dlr.de.
† German Aerospace Center DLR.
‡ University of Cologne.

(1) Xu, Y. *Ferroelectric materials and their applications;* North-Holland: Amsterdam, 1991.
(2) Günter, P. *Nonlinear Optical Effects and Materials;* Springer: Berlin, 1999.
(3) Miller, R. C. *Phys. Rev.* **1964**, *134*, 1313.
(4) Kurtz, S. K.; Perry, T. T. *J. Appl. Phys.* **1968,** *39*, 3798.
(5) Skipetrov, S. E. *Nature* **2004**, *432*, 285.
(6) Baudrier-Raybaut, M.; Haidar, R.; Kupecek, Ph.; Lemasson, Ph.; Rosencher, E. *Nature* **2004**, *432*, 374.
(7) Wiersma, D. S.; Cavalieri, S. *Nature* **2002**, *414*, 708.
(8) Hüsing, N.; Schubert, U. *Angew. Chem., Int. Ed. Engl.* **1998**, *37*, 23.

10.1021/cm052784r CCC: $33.50
Published on Web 02/18/2006

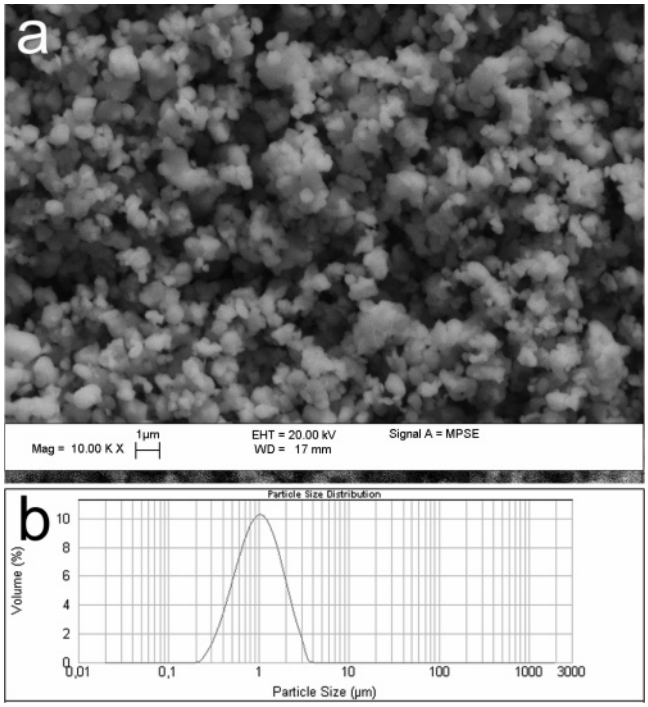

Figure 1. (a) SEM picture of $BaTiO_3$ particles. (b) Particle size distribution as measured with light scattering adding sodium polyphosphate and ultrasound to destroy agglomerates.

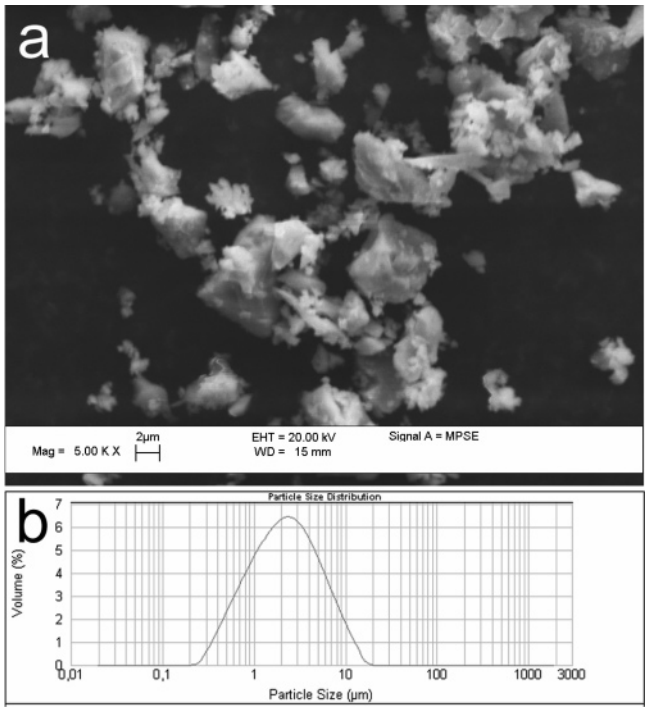

Figure 2. (a) SEM picture of $KNbO_3$ grinded manually to a powder from larger single crystals. (b) Particle size distribution as measured with light scattering adding sodium polyphosphate and ultrasound to destroy agglomerates.

employed laser-light scattering (Malvern Mastersizer 2000). We prepared a water-based dispersion of the powders. To destroy possible agglomerates, we tested several dispersants. Sodium polyphosphate together with an ultrasonic treatment lead to a complete deflocculation and size distributions with a single peak. Figure 1b illustrates the results of the light-scattering measurements from $BaTiO_3$. The size distribution looks symmetric with sizes between 0.3 and 3 μm with a maximum at 1 μm. However, the abscissa is logarithmic, such that the size distribution itself is a log-normal one. Figure 2b shows light-scattering results for the $KNbO_3$ powder. It can be seen that the particles have larger sizes between 0.3 and 12 μm with a maximum at 2.5 μm.

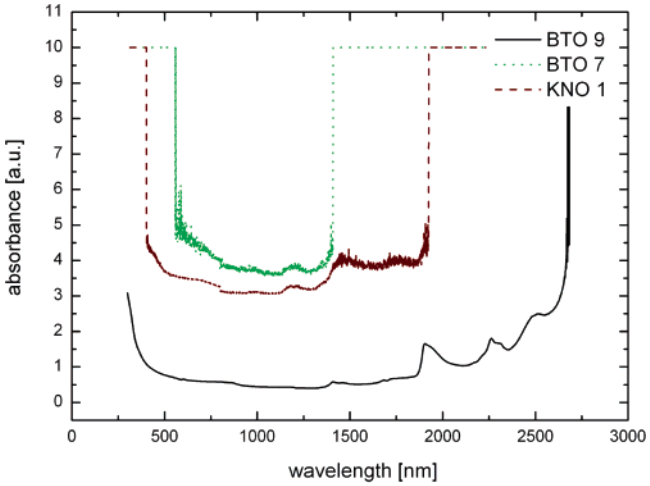

Figure 3. Absorption spectra of the pure waterglass xerogel (BTO9), of a potassium niobat xerogel sample (KNO1), and of a barium titanate xerogel sample (BTO7).

The crystallographic structure of the particles was checked by room-temperature powder X-ray diffraction (XRD) on the Seifert Iso-Debye Flex diffractometer and was characterized with the Jana2000[9] software. The $BaTiO_3$ particles are in the tetragonal phase (*P*4*mm*), while the $KNbO_3$ particles are in the orthorhombic phase (*Amm*2). Both crystal structures are noncentrosymmetric, and thus SHG generation is possible with these powders.

Materials Preparation. The waterglass-based aerogels loaded with ferroelectric particles were prepared by the following method. Sodium waterglass and acetic acid (99.8%), both from Sigma-Aldrich, and deionized water were mixed with molar ratios of 1:44:0.5 (waterglass:water:acetic acid). To distribute the ferroelectric particles into the sol before the gelation process started, we developed a two-step procedure. Two separate solutions are prepared which alone do not form a gel. On mixing these solutions, the gelation process starts. The first solution was mixed from 1.09 g water and 0.58 g waterglass. The second solution contains 1.41 g water and 0.09 g acetic acid. In the waterglass solution, we dispersed 0.3−3.5 g $BaTiO_3$ or $KNbO_3$ powder (Table 1) either by manually shaking or stirring the solution or by pumping through a specially built high-speed pump.[10] Mixing both solutions initiated the gelation process. Within 15 s, the gelation is finished. The gelation time could be varied by the amount of acetic acid in the range from 10 seconds to 10 minutes. A fast gelation is important to quickly fix the dense particles by the gel network and to prevent them from sedimentation and agglomeration. The wet gel was cut into samples of $L = 2$ mm thickness. These wet gels were either dried supercritically to yield an aerogel[8] using the well-known solvent exchange procedure[8] or dried under ambient

(9) Petricek, V.; Dusek, M. *The crystallographic computing system JANA2000*; Institute of Physics: Praha, 2000.
(10) Brück, S.; Reuss, M.; Richter, H. E.; Klein, H.; Haubner, P.; Ratke, L. *Microgravity Sci. Technol.* **2005**, *16*, 31.

Table 1. Amount of $BaTiO_3$ (BTO) or $KNbO_3$ (KNO) Powder (in Percent by Weight [wt %]) Embedded in a 3 mL Liquid Waterglass Xerogel (WG) Solution[a]

sample	powder [g]	WG solution [g]	$BaTiO_3$ [wt %]
BTO1	3,50 ± 0,05	3,2 ± 0,1	52
BTO2	3,00 ± 0,05	3,2 ± 0,1	48
BTO3	2,50 ± 0,05	3,2 ± 0,1	44
BTO4	2,00 ± 0,05	3,2 ± 0,1	38
BTO5	1,50 ± 0,05	3,2 ± 0,1	32
BTO6	1,00 ± 0,05	3,2 ± 0,1	24
BTO7	0,50 ± 0,05	3,2 ± 0,1	14
BTO8	0,40 ± 0,05	3,2 ± 0,1	11
BTO9	0	3,2 ± 0,1	0
KNO1	0,35 ± 0,05	3,2 ± 0,1	10

[a] KNO1 and BTO7 have the same volume concentrations. Without powder, these xerogels have a density of 1.3 g/cm^3 and a specific surface of 270 m^2/g.

conditions yielding a xerogel. Here, our mixed xerogels have a density of 1.3 g/cm^3 and a specific surface of 270 m^2/g. The specific surface is measured by the BET method (Beckmann & Coulther, SA3100). A few samples were also prepared by mixing the two solutions with a high-speed pumping device and by finishing the gelation under reduced gravity conditions of a parabolic flight to avoid sedimentation of the dense particles (details are described in ref 10). These gels were dried supercritically.

Optical Measurements. The optical transmission/absorption of the samples was measured using a conventional two-beam spectrometer (CARY). Figure 3 shows the result for a waterglass xerogel (BTO9) without powder. This absorption spectrum is typical for waterglass xerogels, exhibiting a transparency range of 400−2500 nm. The transparency at 1064 and 532 nm is especially sufficient for second-harmonic generation.

For the second-harmonic generation, we used the 1064-nm pulse of a Nd:YAG laser, which has a full width at half-maximum of 6 ns, a beam diameter of 5 mm, and a regulable input energy from 0 to 80 mJ. The generated SHG signal was measured in transmission with a silicon diode with a detection area of 0.5 mm^2 (the transmitted IR beam was filtered by an IR mirror and a 532 nm interference filter). The energy of the incoming IR beam was measured with a reference diode. The distance between the sample and the Si-diode was 100 mm.

Results and Discussion

First of all, the most important result is that aerogels with $BaTiO_3$ and waterglass xerogels with $BaTiO_3$ and $KNbO_3$ exhibit a strong frequency doubling effect. The naked eye immediately observes a diffusive green light emitted from the whole sample on illumination with infrared light, as sketched schematically in Figure 4a. Figure 4b shows a photograph of the generated diffuse green light. For powder samples, the SHG source behaves like an isotropic planar radiation source[4] if the average particle size r is smaller than the layer thickness L and much smaller than the laser beam diameter D, a condition well fulfilled in our setup ($L = 2$ mm, $D = 5$ mm). Thus, the transmitted energy is only a small portion of the total diffuse energy, and one has to be careful in comparing different materials if only measuring a part of the total generated SHG energy. However, in our

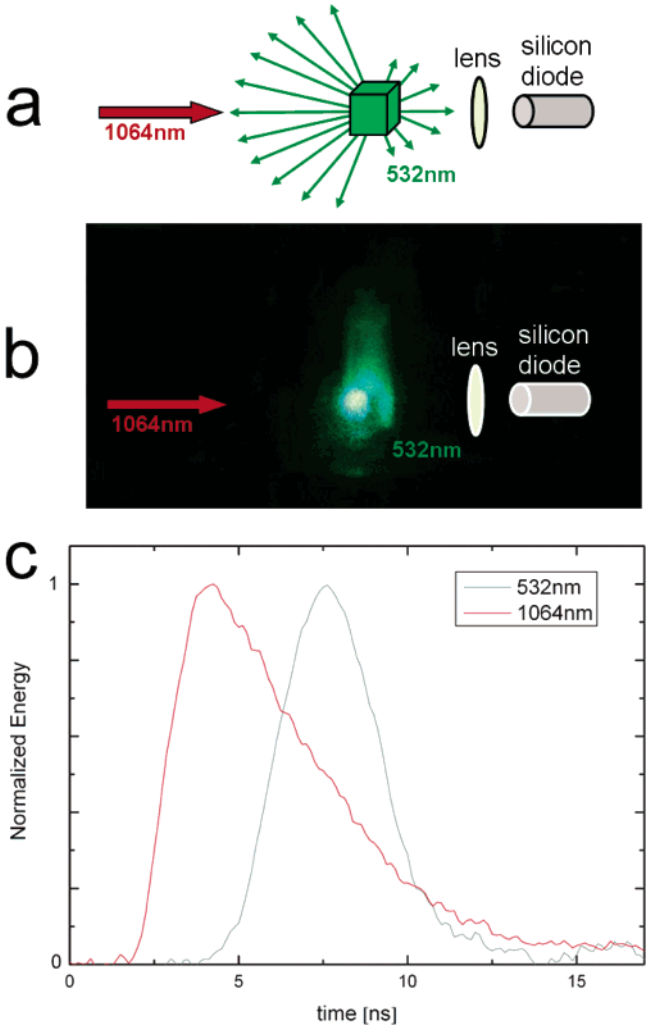

Figure 4. (a) Schematics of second-harmonic generation and detection in aerogels and xerogels. (b) Photograph of generated green light upon illumination with 1064 nm in the xerogel sample loaded with $BaTiO_3$ particles (BTO7). (c) Normalized energy of the excitation (1064 nm) and SHG-signal (532 nm) of $BaTiO_3$ powder embedded in a xerogel (BTO7). This figure looks similar for all aerogel and xerogel samples loaded with $BaTiO_3$ or $KNbO_3$ powder (Table 1).

case, the two samples $BaTiO_3$ and $KNbO_3$ have almost identical refractive indices and hence the same Rayleigh scattering properties, so we can restrict ourselves to the measurement of the transmitted light. Figure 4c shows the original 1064 nm pulse from the laser together with the generated SHG-pulse observed behind the sample loaded with $BaTiO_3$ (BTO7). As expected, the line width of the stimulating infrared beam is twice that of the excited one (6 ns (1064 nm) to 3 ns (532 nm)).[10] Also, the IR pulse has a long tail and is asymmetric, whereas the generated green pulse is highly symmetric. We assume that the origin of this decrease in pulse shape is given by the low green intensity so that only the top of the pulse amplitude of the IR pulse is detected for the SHG signal. We did not observe any SHG signal of the pure xerogels and aerogels on pulsed infrared illumination, so the matrix does not exhibit nonlinear optical properties and the ferroelectric particles inside the transparent gel matrix are responsible for the observed SHG signal.

Second, we have measured the generated SH-energy as a function of $BaTiO_3$ particle concentration in the xerogel matrix (see Table 1 and Figure 5). The amplitude of the

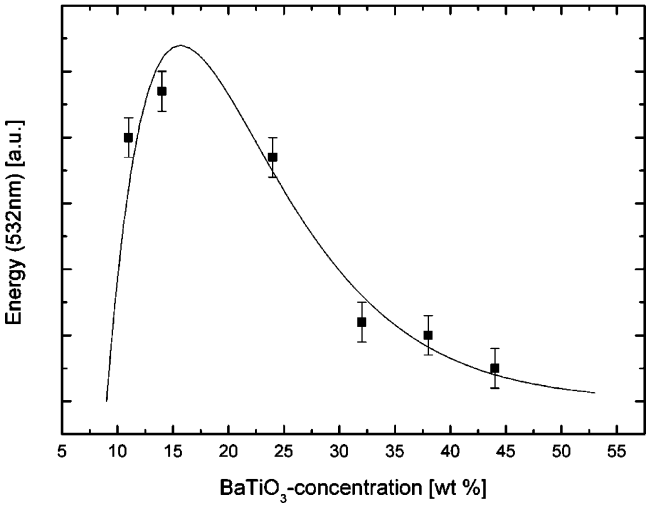

Figure 5. Transmitted SHG-energy as a function of the $BaTiO_3$-concentration in a xerogel.

transmitted SHG-signal shows a distinct dependence on the $BaTiO_3$ concentration inside the gel body. It first increases with the particle concentration up to a maximum at 16 wt % and decreases with further increase of the particle concentration. This characteristic behavior can be explained on the basis of two oppositely acting contributions. On one hand, the increase in particle concentration naturally leads to an increase of the generated SH-energy; on the other hand, it also leads to a decrease in the overall xerogel transparency and to an increase of the diffuse scattering. This behavior can be modeled using a simple scattering approach

$$E(n) \sim n \cdot e^{-n\alpha L}$$

with the energy E, the number of particles per volume n, the extinction coefficient α, and the sample thickness L.

Third, we have detected the linear increasing part of the transmitted SHG signal as a function of the incident IR energy in the range 20−70 mJ in both materials (Figure 6). The $BaTiO_3$ (BTO7) and the $KNbO_3$ (KNO1) xerogels have the same volume concentration. A linear fit to the data with $I_{532} = a \cdot I_{1064} + b$ allows for a comparison of the SHG efficiency between the embedded $BaTiO_3$ and $KNbO_3$ particles. For samples with $BaTiO_3$, we get the parameters $a = (5.6 \pm 0.5)10^{-11}$ and $b = (-0.76 \pm 0.12)$ pJ and for $KNbO_3$ samples we have $a = (6.4 \pm 0.3)10^{-9}$ and $b = (-61 \pm 8)$ pJ. The slopes of both samples differ by 2 orders of magnitude so that for particles of $BaTiO_3$ the SHG-efficiency is 100 times smaller than for $KNbO_3$ in our transmission setup. The energies measured in transmission are much smaller than the totally generated SHG energy. The total energy emitted in all directions can be estimated from the ratio of the surface of a sphere around the sample having a radius of the distance between sample and detector and the detector area as 4π (100 mm)/0.5 mm^2. This yields a factor of 10^5. The total energy is thus much larger than the measured one and amounts to a few microjoules in the case of samples with $KNbO_3$ particles.

In general, it is well-known that the energy of the SHG signal generated in single crystals increases quadratically with the incident energy. However, it was shown by Morozov and co-workers[11] that a different relation holds for nonlinear optical crystals with a random domain distribution. Here, at low incident energies, a linear relation between incident and frequency doubled energy occurs which then gradually changes into the usual quadratic dependence at higher incident energies. Hence, our randomly distributed polar axes of the particles correspond to a random domain distribution, so that we are working in this low-intensity linear regime. From single crystal and powder measurements relative to standards such as quartz and KDP, it is known that $KNbO_3$ has a higher SHG efficiency than $BaTiO_3$ of about a factor of 5−15, depending on the actual setup.[4,12,13] The larger difference in our setup is most probably due to the different particle size of the embedded particles. The $KNbO_3$ particles have a medium size of 3 μm while the $BaTiO_3$ samples have sizes around 1 μm. Since the SHG efficiency scales with the particle size (crystal length), as long as it is shorter than the coherence length, this leads to an additional factor of at least 3, explaining the higher efficiency observed in $KNbO_3$ samples.

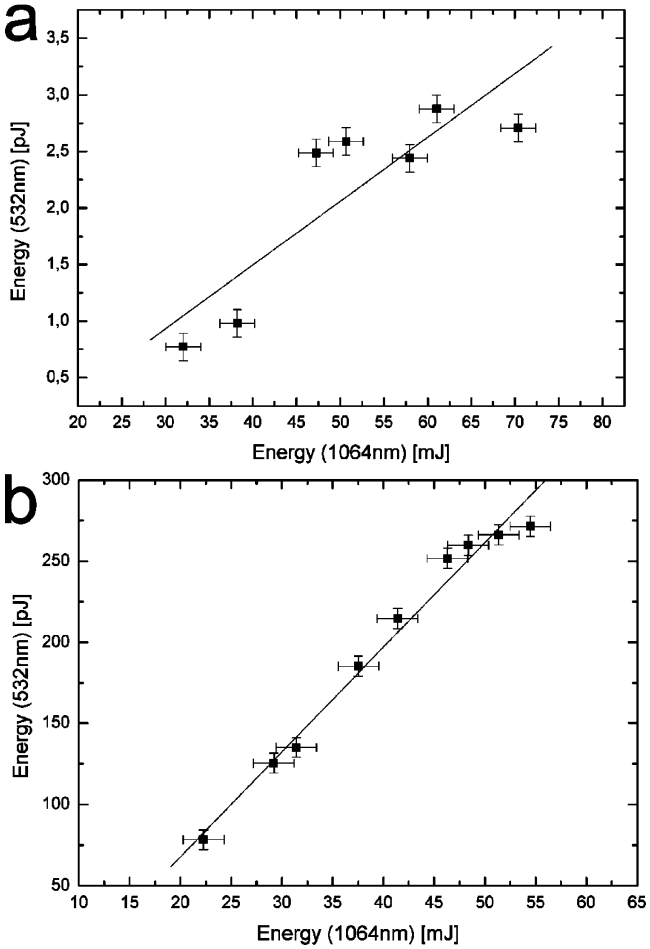

Figure 6. SHG-energy as a function of excitation energy of samples with $BaTiO_3$ (a) and $KNbO_3$ (b) powders embedded in a xerogel. The amounts are 0,5 g $BaTiO_3$ (BTO7) and 0,35 g $KNbO_3$ (KNO1) in a 3,2 g aerogel solution.

(11) Morozov, E. Yu.; Kaminskii, A. S.; Yusupov, D. B. *JETP Lett.* **2001**, *73*, 647.
(12) Zhao, T.; Chen, Z.-H.; Chen, F.; Shi, W.-S.; Lu, H.-B.; Yang, G.-Z. *Phys. Rev. B* **1999**, *60*, 1697.
(13) Xue, D.; Zhang, S. *Chem. Phys. Lett.* **1998**, *291*, 401.

Finally, the aerogel and xerogel samples suffer no damage from the pulse energy of 60 mJ (fwhm 6 ns, 10 Hz, 5 mm beam diameter), and with an energy of 20 mJ, a clear SHG signal is already detectable.

Conclusion

In conclusion, we have presented new types of composite ferroelectric aerogels and xerogels that exhibit nonlinear optical properties, especially second-harmonic generation, whereby the particle sizes are in the range of the pump wavelength (1 μm). This class of composite materials might be useful for applications since the aerogels can be manufactured in any desired shape. An obvious improvement would be the adaptation of the refractive index of the aerogel matrix to that of the embedded ferroelectric particles, which would yield a much higher SHG signal in forward direction.[4] A similar enhancement can be expected by applying an electric field during the gelation of the composites to align the ferroelectric particles in the matrix.

Acknowledgment. We thank Dr. D. Rytz, FEE Forschungsinstitut für mineralische und metallische Werkstoffe Edelsteine, Struthstr. 2, D-55743 Idar-Oberstein, Germany, for providing the $KNbO_3$ crystals.

CM052784R